BIOLOGY OF REPRODUCTION **81,** 302–309 (2009)
Published online before print 25 February 2009.
DOI 10.1095/biolreprod.108.073221

Cloning, Characterization, and Expression Analysis of the Novel Acetyltransferase Retrogene *Ard1b* in the Mouse[1]

Alan Lap-Yin Pang,[2,3] Stephanie Peacock,[3] Warren Johnson,[3] Deborah H. Bear,[3] Owen M. Rennert,[3] and Wai-Yee Chan[3,4]

Laboratory of Clinical Genomics,[3] Eunice Kennedy Shriver National Institute of Child Health and Human Development, National Institutes of Health, Bethesda, Maryland
Department of Pediatrics,[4] Georgetown University, Washington, District of Columbia

ABSTRACT

N-alpha-terminal acetylation is a modification process that occurs cotranslationally on most eukaryotic proteins. The major enzyme responsible for this process, N-alpha-terminal acetyltransferase, is composed of the catalytic subunit ARD1A and the auxiliary subunit NAT1. We cloned, characterized, and studied the expression pattern of *Ard1b* (also known as *Ard2*), a novel homolog of the mouse *Ard1a*. Comparison of the genomic structures suggests that the autosomal *Ard1b* is a retroposed copy of the X-linked *Ard1a*. Expression analyses demonstrated a testis predominance of *Ard1b*. A reciprocal expression pattern between *Ard1a* and *Ard1b* is also observed during spermatogenesis, suggesting that *Ard1b* is expressed to compensate for the loss of *Ard1a* starting from meiosis. Both ARD1A and ARD1B can interact with NAT1 to constitute a functional N-alpha-terminal acetyltransferase in vitro. The expression of ARD1B protein can be detected in mouse testes but is delayed until the first appearance of round spermatids. In a cell culture model, the inclusion of the long 3′ untranslated region of *Ard1b* leads to reduction of luciferase reporter activity, which implicates its role in translational repression of *Ard1b* during spermatogenesis. Our results suggest that ARD1B may have an important role in the later course of the spermatogenic process.

gametogenesis, gene regulation, meiosis, spermatogenesis, testis

INTRODUCTION

N^{α}-terminal acetylation is one of the most common protein modifications occurring on eukaryotic proteins. About 90% of mammalian proteins are N-terminally acetylated at the α-amino group [1]. This cotranslational modification process is catalyzed by N^{α}-terminal acetyltransferase (NAT). Despite its common occurrence, the biological significance of this modification is generally unknown, except for the belief that N^{α}-acetylated proteins are thermally more stable and resistant to protease action [2].

Three types of NATs have been identified in yeast [2, 3]. NatA, the major NAT, consists of the catalytic subunit Ard1p and the auxiliary subunit Nat1p that anchors the enzyme complex to ribosomes [4]. The similar phenotypic changes in *nat1*$^{-}$ and *ard1*$^{-}$ (arrest defective 1^{-}) mutants, which include slow growth, temperature sensitivity, and derepression of the silent mating locus *HMLalpha*, failure to enter G_0 phase of the cell cycle and consequently to sporulate, indicate that these two proteins function in the same cellular process [5–7], and these two subunits were proven to interact to form an active NAT [7]. Similar findings were later obtained in mammalian cells. Mouse NAT activity can be detected only when NAT1 and ARD1A heterodimer is formed [8]. Similarly, human NAT1 and ARD1A proteins interact to display NAT activity [9]. Both NAT1 and ARD1A family members are evolutionarily conserved [10, 11]. The existence of a similar system for N^{α}-terminal acetylation from yeast to higher eukaryotes suggests that this cotranslational modification process is essential for normal cellular function. Notably, removal of either NAT1 or ARD1A by RNA interference (RNAi) in human cell lines triggers apoptosis [12]. To our knowledge, the in vivo substrate specificities of NATs, particularly in higher eukaryotes, have not been characterized. Eukaryotic proteins with serine, alanine, methionine, glycine, and threonine at N-termini tend to be the preferred substrates for N^{α}-acetylation, but there is no consensus sequence motif or dependence on amino acid residue for signaling N^{α}-acetylation of a particular protein [2]. An isoform of mouse ARD1A was shown to directly acetylate hypoxia-inducible factor 1-α (HIF1A) at a specific internal ε-amino group to promote its degradation [13]. In another study [14], human ARD1A was implicated to promote lung cancer cell proliferation by directly acetylating and activating β-catenin. These results suggest that ARD1A may display different substrate specificity in the presence or absence of NAT1. Recently, an isoform of human *ARD1A* (*ARD1B*) was identified by a database search [11]. Despite the implication of the expression of a homologous transcript in rodents, the cloning of such transcripts has not been attempted, to our knowledge.

Spermatogenesis is a highly orchestrated developmental process of male germ cells. Spermatogonial stem cells can either undergo mitosis for self-renewal or commit themselves to meiosis and subsequently differentiate into spermatozoa [15]. It is believed that the highly organized nature of the spermatogenic process is regulated by a sophisticated mechanism that involves a concerted change in the gene expression program in a developmentally regulated manner [16–20]. However, many of the genes involved remain uncharacterized. During a screening of genes that are differentially expressed between meiotic and postmeiotic male germ cells [20], an expressed sequence tag (EST) was found to be preferentially

[1]Supported by the Intramural Research Program of Eunice Kennedy Shriver National Institute of Child Health and Human Development, National Institutes of Health. The nucleotide sequence of *Ard1b* (*Ard2*) transcript had been deposited in GenBank under the accession number EU192141.
[2]Correspondence: Alan Lap-Yin Pang, Laboratory of Clinical Genomics, Eunice Kennedy Shriver National Institute of Child Health and Human Development, National Institutes of Health, Bethesda, MD 20892. FAX: 301 480 4579; e-mail: panga@mail.nih.gov

Received: 29 August 2008.
First decision: 23 September 2008.
Accepted: 10 February 2009.

eISSN: 1259-7268 http://www.biolreprod.org
ISSN: 0006-3363

expressed in pachytene spermatocytes. We extended this EST to its entirety and identified the transcript (designated as *Ard1b*) as a novel homolog of the mouse *Ard1a* gene. We further characterized the function and studied the expression of *Ard1b*. Our results suggest that *Ard1b* is a novel testis-predominant retrogene of *Ard1a*, which is preferentially expressed in male meiotic germ cells and is subject to translational regulation during spermatogenesis.

MATERIALS AND METHODS

Testicular Cell Isolation

Protocols for the use of mice were approved by the Georgetown University Animal Care and Use Committee. Male germ cell isolation by STAPUT technique from BALB/c mice was performed as described previously [20]. Briefly, type A spermatogonia and Sertoli cells were isolated from testes of 6-day-old mice, while pachytene spermatocytes and round spermatids were isolated from testes of 60-day-old animals. Purities of the different testicular cells isolated are at least 90% and have been described previously [20].

Total RNA Preparation

Total RNA samples from germ cells were extracted using Trizol reagent (Invitrogen, Carlsbad, CA) and the RNeasy Mini kit (Qiagen, Germantown, MD). RNA integrity and concentration were monitored by optical densities at 260 nm and 280 nm and by use of the Bioanalyzer 2100 (Agilent Technologies, Waldbronn, Germany). Total RNA samples of different mouse tissues were obtained from Ambion (Austin, TX).

Molecular Cloning of Ard1b

The EST BG069933, which is expressed in pachytene spermatocytes [20], represented the 3′ reading of the National Institute on Aging (Bethesda, MD) mouse 15K cDNA clone H3082G03. Another EST (BG082949) was found to represent the 5′ reading of the same cDNA clone. The whole insert was sequenced (Table 1), and the genuine 5′ and 3′ ends of the putative transcript were isolated by performing RNA ligase-mediated rapid amplification of cDNA ends (RLM-RACE) using the GeneRacer kit (Invitrogen). For the preparation of RLM-RACE-ready cDNA, 1 μg total RNA from pachytene spermatocytes was used. Amplified DNA fragments were cloned into pCR4-TOPO vector (Invitrogen) and verified by DNA sequencing (Table 1). The expression of an intact *Ard1b* transcript was confirmed by RT-PCR using primers flanking the putative 5′ and 3′ ends of the transcript (data not shown). The putative open reading frame (ORF) of *Ard1b* was predicted in silico using ORF Finder from GenBank (National Center for Biotechnology Information [NCBI], Bethesda, MD). Genomic structures of *Ard1a* and *Ard1b* were obtained by a BLAST(N) search of the NCBI mouse genome (http://www.ncbi.nlm.nih.gov/genome/guide/mouse/) and using the Ensembl genome browser (http://www.ensembl.org/Mus_musculus/index.html).

Expression Analysis of Ard1a *and* Ard1b *by RT-PCR*

Total RNA samples from different mouse tissues and isolated testicular cells were treated with DNase I (Invitrogen) and examined using the Bioanalyzer 2100. First-strand cDNA was synthesized using SuperScript II RT and random hexamers (Invitrogen) as described previously [20]. Gene-specific PCR primers for *Ard1a* (X-F: 5′-ATGAACATCCGCAATGCTA-3′; X-R: 5′-CTAGGAGGCAGAGTCAGA-3′) and *Ard1b* (CDS-F: 5′-ATGAACATCCGCAATGCCC-3′; CDS-R: 5′-CTAGGAGATGGAATCCAAGTCCTC-3′) were designed using Primer Express version 2.0 (Applied Biosystems, Foster City, CA). Primer mix for β-actin (*Actb*), as a component of the QuantumRNA ACTB internal standards kit, was purchased from Ambion. The PCR was performed in the presence of 1 μl 5-fold diluted first-strand cDNA product, 2.5 mM $MgCl_2$, 0.5 mM deoxyribonucleotide triphosphates, 0.5 μM forward and reverse primers, and 1 U Platinum *Taq* DNA polymerase (Invitrogen). The PCR was performed as follows: 94°C for 5 min, followed by 30 cycles of 94°C for 30 sec, 54°C (*Ard1a*) or 58°C (*Ard1b*) for 35 sec, and 72°C for 1 min. After temperature cycling, an extra extension of 7 min at 72°C was performed. The PCR profile for *Actb* is similar, except for the reduction of temperature cycling to 27 times and the use of an annealing temperature at 60°C. The PCR products were analyzed on 1.5% Tris acetate-edetic acid agarose gel stained with ethidium bromide and visualized by UV transillumination.

TABLE 1. Primers used for cloning and sequencing *Ard1b* gene.

Primer type	
Primers for sequencing H3082G03 cDNA clone	Primer name
5′-TTGTAATACGACTCACTATAGG-3′	T7
5′-AGCTATTTAGGTGACACTATAG-3′	SP6
5′-TAAAAGTAGGTGTAGGCAAAGGGC-3′	2-F
5′-CTTACAAATCGGCCCCAGTG-3′	3-F
5′-CAGCTTTCTAACATCTGTCTCCAGG-3′	5-F
5′-GCAGCAGCCTACCGAGTTTGG-3′	6-F
5′-ACTCGAGTGAACCCTGTTTTGTC-3′	7-F
5′-CCGACTAGTAATGGTCATGAACATC-3′	8-F
5′-GCTCTTATCTCCAAGGGAAGAACAG-3′	2-R
5′-GAAGGGGCGTGAGTCACTCTAC-3′	3-R
5′-TGCTTCTCTGCCATCAGCAGC-3′	4-R
5′-CAGCTTACTAGAGACTCGGTGTGC-3′	5-R
5′-GGAAGGACCGAGGACTAGGTTG-3′	6-R
5′-GGTCATCAGCTGCTTAATGTCAG-3′	7-R
Gene-specific primer for 3′ RACE	
5′-CCGACTAGTAATGGTCATGAACATC-3′	8-F
Gene-specific primers for 5′ RACE	
5′-GGAAGGACCGAGGACTAGGTTG-3′	6-R
5′-GGTCATCAGCTGCTTAATGTCAG-3′	7-R
5′-AACACAGGACCACGGCAAAC-3′	H3exonR
Primers used for sequencing DNA fragments cloned into TOPO vector	
5′-GGAAACAGCTATGACCAT-3′	M13-R
5′-GTAAAACGACGGCCAGTG-3′	M13–20
5′-TTGTAATACGACTCACTATAGG-3′	T7
5′-TGAAGGAACACCTCAGCGC-3′	H3exonF
5′-AACACAGGACCACGGCAAAC-3′	H3exonR

Protein-Protein Interaction by Coimmunoprecipitation

Expression vectors for MYC-tagged NAT1 and HA-tagged ARD1A (CS2+MT-mNAT1 and CS2+mARD1/HA) were gifts from Roderick A. Corriveau (Department of Cell Biology and Anatomy, Louisiana State University, Baton Rouge, LA). To express a C-terminal hemagglutinin epitope (HA)-tagged ARD1B, the *Ard1b* ORF was amplified from pachytene spermatocyte cDNA using *Pfu* Turbo DNA polymerase (Stratagene, La Jolla, CA) and gene-specific primers (KpnI-mArd1b-ORF-F: 5′-*TAGGGC*GGTACC ATGAACATCCGCAATG-3′; KpnI-mArd1b-ORF-R: 5′-*TAGGGC*GGT ACCGGAGATGGAATCCAAG-3′) with *Kpn*I sites (underlined) incorporated at their 5′ ends. The PCR product was cloned into ZeroBlunt pCR4-TOPO vector (Invitrogen) and verified by DNA sequencing. Correct clones were then digested with *Kpn*I to release the *Ard1b* ORF for subcloning into phCMV3 vector (Genlantis, San Diego, CA) to generate the expression vector phCMV3-Ard1b/HA. Chinese hamster ovary (CHO)-K1 cells from ATCC (Manassas, VA) were seeded at 1×10^5 cells/well in a six-well plate. Cotransfection of CHO-K1 cells with MYC-NAT1 and ARD1A-HA or ARD1B-HA expression vectors (500 ng each/well) was performed using FuGENE 6 transfection reagent (Roche Applied Bioscience, Indianapolis, IN). Forty-eight hours later, cells were washed twice with cold Hanks balanced salt solution and disrupted by cell lysis buffer (50 mM Tris-HCl [pH 7.6], 150 mM NaCl, and 1% NP-40) in the presence of 1× Halt protease inhibitor cocktail and 5 mM edetic acid (Pierce, Rockford, IL). Cell lysates were passed through a 23-gauge needle 10 times, pooled, and incubated on ice for 30 min with occasional mixing. Soluble fractions were harvested after spinning at 18 000 × *g* at 4°C for 15 min. Protein content was determined by bicinchoninic acid protein assay (Pierce). In each coimmunoprecipitation experiment, 500 μg cell lysate was first precleared with 50 μl TrueBlot anti-rabbit IgG beads (eBioscience, San Diego, CA) on ice for 30 min with occasional mixing. Five micrograms of rabbit anti-HA antibody SG77 (Zymed, San Francisco, CA) or normal rabbit IgG (Santa Cruz Biotechnology, Santa Cruz, CA) was added to the precleared lysate and incubated on ice for 2 h. Subsequently, 50 μl TrueBlot anti-rabbit IgG beads was added, and incubation was continued at 4°C overnight with constant agitation. The immunoprecipitate was washed three times with 500 μl cold cell lysis buffer and resuspended in 50 μl 2× SDS-PAGE loading buffer (Quality Biological, Gaithersburg, MD) with 5% β-mercaptoethanol and heated at 95°C for 5 min. Target proteins were revealed from the immunoprecipitates by Western blotting. Primary antibodies (1:5000) included anti-MYC antibody produced from mice (Invitrogen) or chicken (Abcam, Cambridge, MA) and rabbit anti-HA (Zymed). Secondary antibodies included horseradish peroxidase (HRP)-conjugated goat anti-mouse IgG (BioRad, Hercules, CA) and goat anti-chicken IgY (Abcam), both used at 1:10 000, and goat anti-rabbit TrueBlot

(eBioscience) at 1:1000. SuperSignal West Pico chemiluminescent substrate (Pierce) was used for signal detection. Membranes were regenerated by incubating in Restore Western blot stripping buffer (Pierce) at room temperature for 30 min and rinsing with 1× PBS plus 0.05% Tween 20 (PBST) solution.

NAT Assay

The procedure for NAT assay was adopted from previous studies [8, 9] with minor modifications. NAT1, ARD1A-HA, and ARD1B-HA proteins were in vitro translated from pT7-mNAT1 and pBS-ARD1/HA (gifts from Roderick A. Corriveau, Department of Cell Biology and Anatomy, Louisiana State University) and phCMV3-Ard1b/HA expression vectors separately using the TNT T7 Quick Coupled Transcription/Translation System (Promega, Madison, WI) at 30°C for 90 min. Subsequently, 20 μl in vitro-translated ARD1A-HA or ARD1B-HA was constituted to a volume of 200 μl with 1× PBS in the presence or absence of 100 μl in vitro-translated NAT1. The HA-tagged protein complexes were immunoprecipitated and washed as already described. The NAT assay was performed by incubating the immunoprecipitate at 37°C for 2 h in a reaction containing 136 μl 0.2 M K_2HPO_4 (pH 8.1), 1 μCi [^{3}H]acetyl-coenzyme A (CoA) (152 GBq/mmol; Amersham Biosciences, Piscataway, NJ), and 10 μl 0.5 mM human adrenocorticotropic hormone (ACTH 1–24; Calbiochem, Gibbstown, NJ) with constant agitation. Afterward, 130 μl supernatant was applied to 150 μl 1:1 (v/v) slurry of SP Sepharose in 0.5 M acetic acid (Sigma, St. Louis, MO). The resin was washed three times with 1 ml 0.5 M acetic acid, rinsed once with 300 μl methanol, and resuspended in 75 μl 1× Tris-buffered saline for scintillation counting.

Antibody Production

A monospecific polyclonal antibody targeting a 15-amino acid peptide sequence (DAGEACLPKNPTSKD), which corresponds to amino acids 184–198 of the putative ARD1B ORF, was prepared by immunizing New Zealand white rabbits (Open Biosystems, Huntsville, AL). Antisera were pooled for affinity purification on an immunogen-immobilized Sepharose column.

Expression Analysis of ARD1A and ARD1B by Western Blotting

Twenty micrograms of total testicular protein extracts from mice of different ages (Zyagen, San Diego, CA) were loaded per lane in 10% SDS-PAGE. Proteins were transferred to 0.2-μm polyvinylidene fluoride membrane and blocked in blocking solution (PBST plus 5% nonfat dried milk) at room temperature for 1 h. Primary antibody in blocking solution was added, and the membrane was gently agitated at 4°C overnight. After washing with 1× PBST solution, secondary antibody in blocking solution was added, and the mixture was gently shaken at room temperature for 1 h. Immunoreactivity was detected by SuperSignal West Pico chemiluminescent substrate and film exposure. Primary antibodies used were chicken anti-ARD1A (1:5000; GenWay Biotech, San Diego, CA), rabbit anti-ARD1B (1:2500), and mouse anti-β-actin (1:20 000; Sigma). The HRP-conjugated secondary antibodies included goat anti-chicken IgY (1:20 000; Abcam), goat anti-rabbit IgG (1:10 000; BioRad), and goat anti-mouse IgG (1:20 000; BioRad).

Construction of Luciferase Reporter Plasmids for Ard1b 3′ Untranslated Region

The whole 3′ untranslated region (UTR) of *Ard1b* was amplified by HiFidelity Platinum *Taq* DNA polymerase (Invitrogen) in the presence of cDNA prepared from mouse pachytene spermatocytes and primers XbaI-mArd1b-3-UTR-F (5′-TCTAGAAGCATTTCCTGAGCATCGC-3′) and XbaI-mArd1b-3-UTR-R (5′-TCTAGAGCACTATAAATAAACATTTTTATTG TATG-3′). The PCR product was cloned into pCR4-TOPO vector, verified by DNA sequencing, and subcloned into pGL4.13[*luc2*/SV40] vector (Promega) to generate the *Ard1b* 3′ UTR reporter construct.

Transient Transfection and Luciferase Reporter Assay

Mouse cell line GC-2spd(ts) (SV40 large T antigen-transfected spermatocytes) was purchased from ATCC and cultured under the recommended conditions. The cells were seeded to 24-well plates at a density of 2×10^4 cells/well. The *Ard1b* 3′ UTR reporter construct and parental vector pGL4.13[*luc2*/SV40], which carry the firefly luciferase gene as the reporter gene, were separately transfected into the cells at 100 ng/well using FuGENE 6 transfection reagent. In each transfection, 10 ng reporter plasmid pGL4.73[*hRluc*/SV40] carrying the *Renilla* luciferase gene (Promega) was cotransfected as an internal normalization control. Cells were harvested 2 days later for luminescence measurement using the Dual-Luciferase Reporter Assay System (Promega) in a 20/20^n luminometer (Turner BioSystems, Sunnyvale, CA). Nontransfected cells were included to monitor background luminescence. The activity of the reporter construct was represented by normalizing the firefly luciferase activity to that of *Renilla* luciferase after subtraction of background signal.

Statistical Analysis

Statistical analyses for luciferase reporter activity and NAT activity assays were performed using paired two-tailed Student *t*-test. $P < 0.05$ was considered statistically significant.

RESULTS

Identification of Ard1b and Comparison with Ard1a

The EST BG069933, which is preferentially expressed in pachytene spermatocytes [20], was extended to its entirety by performing 5′ and 3′ RACE. The novel transcript (EU192141) was 3439 base pair (bp) in length and polyadenylated, and it encoded a putative ORF of 657 bp that translated into a protein with 218 amino acid residues. A (BLAST)N search against mouse transcripts revealed a high degree of homology between this ORF and *Ard1a* (NM_019870), the mouse homolog of yeast arrest defective 1, which encodes an evolutionarily conserved catalytic subunit of NAT [5, 8, 11]. We named this novel gene *Ard2*. Subsequent update of the NCBI Unigene cluster identified this gene as *Ard1b*. The amino acid sequence of ARD1B has been found to be highly conserved between primates and rodents [11]. Alignment of the nucleotide and amino acid sequences of their coding regions indicates that *Ard1a* and *Ard1b* share 86% and 77% sequence identity, respectively, with each other (Fig. 1). The major difference between the two polypeptides is limited to the 3′ ends of their coding region. The nucleotide sequence flanking the start codons of these homologs matches the consensus sequence by Kozak [21]. Despite these similarities, the genomic organization between these two genes is totally different. A search of the mouse genome at the NCBI showed that *Ard1b* was composed of two exons and one intron (Fig. 2A) and mapped to the mouse chromosome 5E3 region. Its entire ORF is present within the first exon; the second exon constitutes almost the entire 2.7-kilobase pair (kbp) 3′ UTR of the gene (Fig. 2A). Splicing of *Ard1b* transcripts follows the canonical GT/AG rule at the donor and acceptor sites [22], and it was confirmed by PCR using primers flanking the intron (data not shown). In contrast, *Ard1a* is X-linked, and its ORF spans over eight exons. Unlike *Ard1b*, the 3′ UTR of *Ard1a* is only 85 bp in length (i.e., ~3% that of *Ard1b*).

Expression Analysis of Ard1a and Ard1b

Analysis by RT-PCR was performed to study the expression patterns of *Ard1a* and *Ard1b* in different mouse tissues and isolated testicular cell types (Fig. 2B). Similar to our previous analysis of the EST BG069933 [20], *Ard1b* was restricted to testis and could be detected in the mitotic type A spermatogonia, meiotic pachytene spermatocytes, and postmeiotic round spermatids. No *Ard1b* expression was found in Sertoli cells and other somatic tissues, except for a trace amount in the ovary. For *Ard1a*, it was found to be ubiquitously expressed. As shown in Figure 2B, two PCR products (708 and 799 bp) were detected. The appearance of the longer amplicon was consistent with the expression of an alternatively spliced form that contains a 91-bp insertion in the *Ard1a* coding region [8], which generates a shorter ARD1A protein isoform [13, 23] by

A

```
Ard1a           ATGAACATCCGCAATGCTAGGCCCGAAGACCTGATGAACATGCAGCACTGCAACCTTCTC 60
Ard1b           ATGAACATCCGCAATGCCCGGCCCGACGACCTGATGAACATGCAGCACTGCAACCTGCTC 60
                ****************  ******* ***************************** ***

Ard1a           TGCCTGCCGGAGAACTACCAGATGAAGTACTATTTCTATCATGGCCTCTCTTGGCCCCAG 120
Ard1b           TGCCTGCCGGAGAACTACCAGATGAAGTACTACTTCTACCATGGCCTGTCGTGGCCCCAG 120
                ******************************** ***** ******** ** *********

Ard1a           CTTTCTTACATTGCTGAGGATGAGAATGGGAAGATTGTGGGCTACGTCTTGGCTAAAATG 180
Ard1b           CTCTCCTACATCGCCGAGGATGAGGACGGCAAGATCGTGGGCTATGTCCTGGCCAAGATG 180
                ** ** ***** ** ********* * ** ***** ******** *** **** ** ***

Ard1a           GAAGAGGACCCAGACGATGTGCCCCATGGACATATCACCTCACTGGCTGTGAAGCGTTCC 240
Ard1b           GAGGAGGACCCCGATGATGTCCCCCACGGGCACATCACCTCGCTGGCCGTCAAGCGCTCA 240
                ** ******** ** ***** ***** ** ** ******** ***** ** ***** **

Ard1a           CACCGGCGCCTTGGCCTGGCTCAGAAGCTGATGGACCAGGCCTCTCGAGCCATGATAGAG 300
Ard1b           CACCGGCGCCTCGGCCTGGCCCAGAAGCTCATGGACCAGGCCTCACGGGCGATGATCGAG 300
                ********** ******** ******** ************** ** ** ***** ***

Ard1a           AACTTCAATGCCAAATACGTCTCCCTGCATGTCAGGAAGAGTAACAGGGCCGCCCTGCAT 360
Ard1b           AACTTCGGCGCCAAGTACGTGTCCCTGCACGTCAGGAAGAGCAACAGGGCGGCCCTGCAC 360
                ******   ***** ***** ******** ********** ******** ********

Ard1a           CTCTATTCCAACACCCTCAACTTTCAGATCAGCGAAGTGGAGCCCAAATACTATGCAGAT 420
Ard1b           CTGTATTCTAACACCCTCAACTTCCAGGTCAGTGAGGTGGAACCCAAGTACTATGCTGAT 420
                ** ***** ************** *** **** ** ***** ***** ******** ***

Ard1a           GGGGAAGATGCGTATGCAATGAAGCGGGACCTCACGCAGATGGCTGATGAGCTGAGGCGG 480
Ard1b           GGTGAAGATGCTTACGCCATGAAGCGGGATCTCTCTCAGATGACTGATGAGCTGAGAAGG 480
                ** ******** ** ** *********** *** * ****** *************  **

Ard1a           CACCTGGAGCTGAAGGAAAAGGGCAAGCACATGGTTCTGGCGGCCTTGGAGAACAAAGCG 540
Ard1b           CAGCTGGTGCTGAAGAAGAA---CAGATATGTGGTTCTG--GGCTCCGA----------G 525
                ** **** ******* * **   **   *  ********  ***   *           *

Ard1a           GAGAACAAAGGCAACGTGCTTCTGAGCTCAGGAGAGGCCTGTCGTGAGGAGAAGGGCCTG 600
Ard1b           GAGACCCAGGGCGGCACACTTCCTGATGCTGGGGAGGCCTGCC---TGCCCAAGAACCCC 582
                **** * * ***  *   ****      * ** ******** *    *   ***  **

Ard1a           GCTGCTGAGGATAGTGGTGGGGACAGCAAGGACCTCAGTGAGGTCAGCGAGACCACAGAG 660
Ard1b           ACAAGCAAAGACAGTGG------CAGCAGTGAC---------------------------- 609
                 *     * ** *****      *****  ***

Ard1a           AGCACAGATGTCAAAGACAGCTCAGAGGCCTCTGACTCTGCCTCCTAG 708
Ard1b           AGCACTGATGTCCAGGACAGCTCAGAGGACTTGGATTCCATCTCCTAG 657
                ***** ****** * ************* **  ** **   *******
```

B

```
ARD1A           MNIRNARPEDLMNMQHCNLLCLPENYQMKYYFYHGLSWPQLSYIAEDENGKIVGYVLAKM 60
ARD1B           MNIRNARPDDLMNMQHCNLLCLPENYQMKYYFYHGLSWPQLSYIAEDEDGKIVGYVLAKM 60
                ********:**************************************:***********

ARD1A           EEDPDDVPHGHITSLAVKRSHRRLGLAQKLMDQASRAMIENFNAKYVSLHVRKSNRAALH 120
ARD1B           EEDPDDVPHGHITSLAVKRSHRRLGLAQKLMDQASRAMIENFGAKYVSLHVRKSNRAALH 120
                ****************************************.*****************

ARD1A           LYSNTLNFQISEVEPKYYADGEDAYAMKRDLTQMADELRRHLELKEKGKHMVLAALENKA 180
ARD1B           LYSNTLNFQVSEVEPKYYADGEDAYAMKRDLSQMTDELRRQLVLK-KNRYVVLGSEE--- 176
                *********:**********************:**:*****:* ** *.:::**.: *

ARD1A           ENKGNVLLSSGEACREEKGLAAEDSGGDSKDLSEVSETTESTDVKDSSEASDSAS 235
ARD1B           -TQGGTLPDAGEACLP-KNPTSKDSG-----------SSDSTDVQDSSEDLDSIS 218
                 .:*..* .:****   *. :::***           :::****:****  ** *
```

FIG. 1. Sequence alignment of mouse *Ard1a* and *Ard1b* gene products. The alignment of the ORFs (**A**) of *Ard1a* and *Ard1b* transcripts and polypeptide sequences (**B**) of ARD1A and ARD1B is shown. The region of ARD1A and ARD1B that shows similarity to GCN5-related N-acetyltransferases, a superfamily of enzymes that catalyze the transfer of an acetyl group from acetyl-CoA to primary amine of substrate proteins, is highlighted in gray. Sequence alignment was performed using ClustalW2 (http://www.ebi.ac.uk/Tools/clustalw2/). The asterisk refers to identical nucleotide or amino acid residue, whereas the colon and period refer to conserved and semiconserved substitutions in amino acid residue, respectively, in all sequences in the alignment.

the introduction of an earlier stop codon. Unlike *Ard1b*, the presence of *Ard1a* transcripts in whole testis was barely detected compared with other tissues. In male germ cells, *Ard1a* was predominantly detected in type A spermatogonia; it was marginally detectable in pachytene spermatocytes and round spermatids. The expression patterns of both *Ard1a* and *Ard1b* in the male germ cells are consistent with the mouse spermatogenic gene expression profiling data obtained by other research groups, which are available in the GermOnline database (http://www.germonline.org). In a separate RT-PCR experiment using total RNA samples extracted from whole testes of 1-, 5-, 11-, 15-, 22-, and 60-day-old mice, which signify closely the first appearance of specific types of male germ cells during the first wave of spermatogenesis [24], *Ard1a* expression was predominantly found in 1-, 5-, and 11-day-old mouse testes. Its signal became successively weakened in testis samples from 15-, 22-, and 60-day-old animals. In contrast, *Ard1b* expression in mouse testes displayed an increasing trend, which peaked at 22 days postpartum, when pachytene spermatocytes and round spermatids are both present in the developing testes (data not shown). These data suggest that the expression of *Ard1a* is restricted to premeiotic male germ cells, whereas *Ard1b* is upregulated starting from male meiosis.

ARD1A and ARD1B Can Interact with NAT1 to Constitute a Functional NAT

The high degree of sequence homology between ARD1A and ARD1B implies that they may be functionally homologous to each other. ARD1A is known to interact with NAT1 to

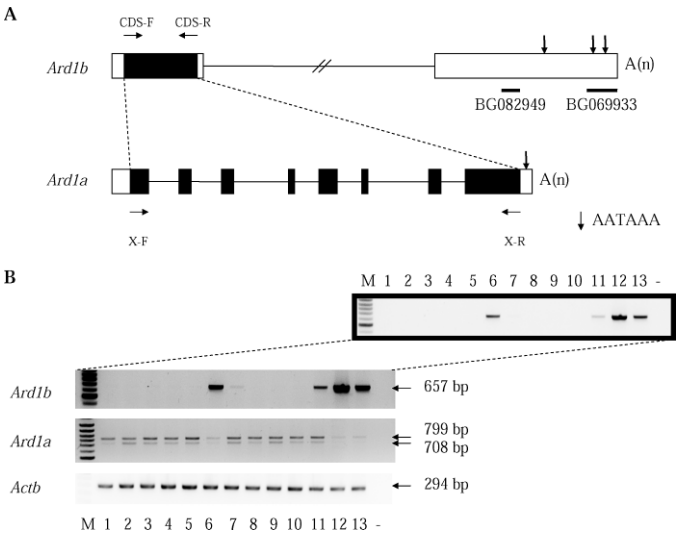

FIG. 2. Genomic structure and expression pattern of *Ard1a* and *Ard1b*. **A**) Genomic organization of *Ard1a* and *Ard1b*. The ORFs are shown in solid black. Vertical arrows indicate the relative positions of canonical polyadenylation signal (AATAAA) in the genes, whereas horizontal arrows indicate the primers used for expression analysis of *Ard1a* and *Ard1b*. The relative positions of the original ESTs (BG082949 and BG069933) representing *Ard1b* are also shown. A(n) represents poly(A) tail. **B**) Analysis of tissue expression pattern of *Ard1a* and *Ard1b* by RT-PCR. Sizes of the expected PCR products are shown. The contrast of the whole panel for *Ard1b* was increased (LabWorks 4.0; UVP BioImaging Systems, Upland, CA) to reveal the presence of PCR product from the mouse ovary (lane 7). The nonenhanced version of the panel (framed) is also included. As determined in our previous study [20], the expression level of *Ard1b* in pachytene spermatocytes and round spermatids is 80-fold and 9-fold, respectively, higher than that in type A spermatogonia. Amplification of β-actin (*Actb*) was performed as an internal control. M, DNA ladder; 1, liver; 2, brain; 3, heart; 4, lung; 5, spleen; 6, testis; 7, ovary; 8, kidney; 9, Embryonic Day 10–12 embryo; 10, Sertoli cells; 11, type A spermatogonia; 12, pachytene spermatocytes; 13, round spermatids; −, no template control.

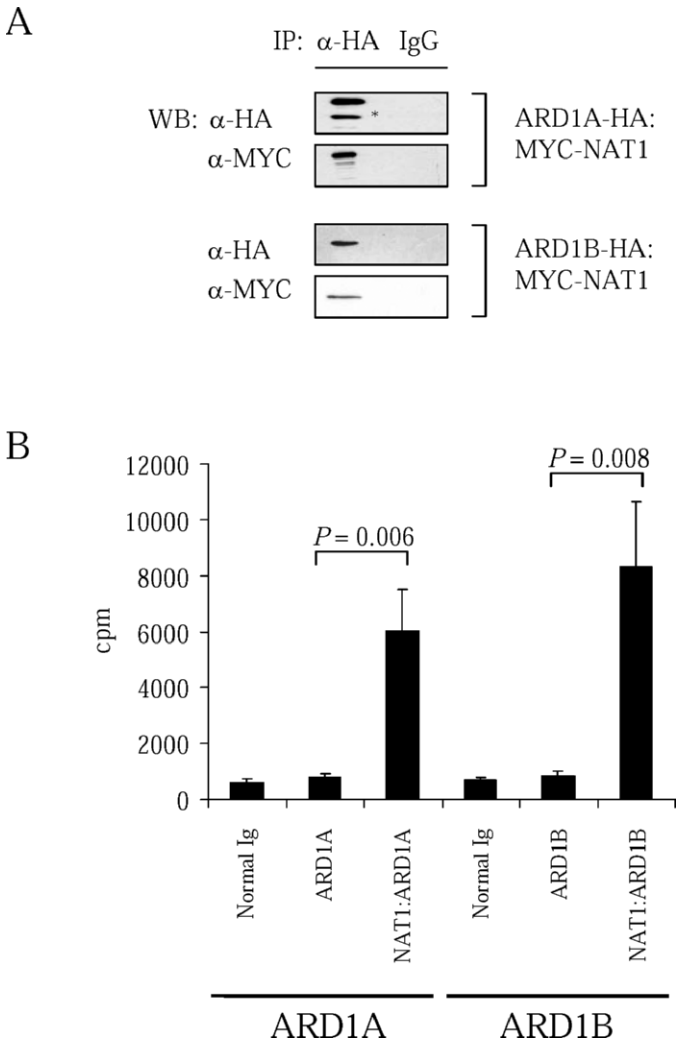

FIG. 3. ARD1B interacts with NAT1 to display NAT activity. **A**) Protein-protein interaction between ARD1B and NAT1. CHO-K1 cells were transiently transfected with HA-tagged ARD1B (ARD1B-HA) and MYC-tagged NAT1 (MYC-NAT1) expression vectors (see *Materials and Methods*). Immunoprecipitation (IP) was performed using rabbit anti-HA antibody and normal rabbit IgG, followed by Western blotting analysis (WB). The presence of ARD1B-HA and MYC-NAT1 in the same immunoprecipitate indicates a physical interaction between the two proteins in mammalian cells. The same study was performed with ARD1A-HA replacing ARD1B-HA. Duplicate experiments were performed, and similar results were obtained. The immunoreactive band denoted by the asterisk represents nonspecific signal or ARD1A-HA proteins that had a partially truncated N-terminal. **B**) NAT assay. In vitro-translated proteins were allowed to interact before immunoprecipitation with rabbit normal IgG or rabbit anti-HA antibody. NAT assay was performed in the presence of [^{3}H]acetyl-CoA and human ACTH 1–24 peptide. Annotation on the x-axis: Normal IgG, ARD1A-HA or ARD1B-HA alone immunoprecipitated by normal IgG; ARD1A or ARD1B, ARD1A-HA or ARD1B-HA alone immunoprecipitated by anti-HA antibody; NAT1:ARD1A or NAT1:ARD1B, the said protein complex immunoprecipitated by anti-HA antibody. Results were compared using paired two-tailed Student *t*-test. Data shown represent the averages of four independent experiments. The error bars represent the SDs of the measurement of radioactivity. cpm indicates the extent of incorporation of the [^{3}H]acetyl group to human ACTH 1–24 peptide in the presence of the different immunoprecipitates.

constitute an active NAT [8]. To demonstrate if the same is true for ARD1B, we first tested whether NAT1 and ARD1B would assemble in mammalian cells. CHO-K1 cells were cotransfected with ARD1B-HA and MYC-NAT1 expression vectors. We used an anti-HA antibody to immunoprecipitate ARD1B-HA from the transfected cell lysates, and the presence of ARD1B-HA was demonstrated by Western blotting analyses (Fig. 3A). When an anti-MYC antibody was used to probe the membrane, MYC-NAT1 protein could also be detected in the same immunoprecipitate, indicating that NAT1 and ARD1B would interact with each other in mammalian cells. The absence of immunoreactivity in the normal rabbit IgG pull-down samples suggests that the immunoprecipitation experiment is specific. After confirming the interaction between NAT1 and ARD1B, we examined if this protein complex would display NAT activity. To avoid any interference from the endogenous NAT1 or ARD1A proteins in mammalian cell cultures, we performed NAT assay with in vitro-translated protein subunits. The in vitro-translated ARD1A-HA or ARD1B-HA and NAT1 were incubated together and subsequently immunoprecipitated. The presence of NAT activity in the immunoprecipitates was measured by transfer of the ^{3}H-acetyl group from [^{3}H]acetyl-CoA to human adrenocortiotropic hormone (ACTH 1–24). As shown in Figure 3B, a background level of NAT activity was detected in the reactions where normal rabbit IgG or rabbit anti-HA antibody was used to immunoprecipitate ARD1A-HA or ARD1B-HA. By contrast, in the presence of NAT1, a significant increase in NAT activity was observed in reactions where ARD1A-HA or ARD1B-HA was immunoprecipitated by anti-HA antibody. The extent of the increase in NAT activity between NAT1/ARD1B-HA and NAT1/ARD1A-HA was similar. Because the expression vector

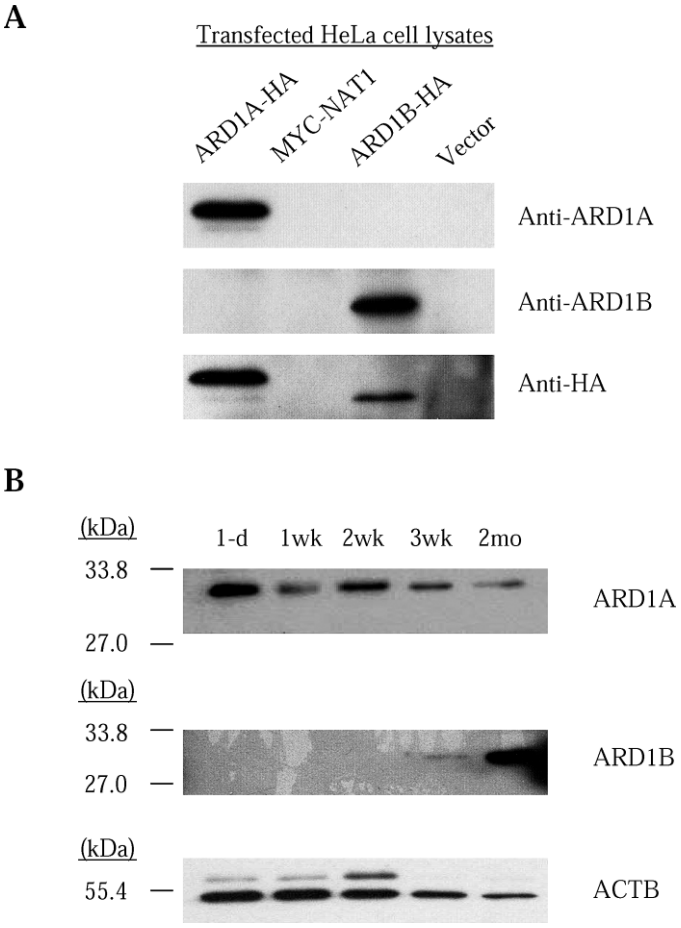

FIG. 4. Developmental expression pattern of ARD1A and ARD1B during spermatogenesis. **A**) Specificity test of antibodies. HeLa cells were first transiently transfected with empty phCMV3 vector (Vector) and expression vectors carrying ARD1A-HA (CS2+mARD1/HA), MYC-NAT1 (CS2+MT-mNAT1), and ARD1B-HA (phCMV3-Ard1b/HA) for 2 days. Western blotting was performed to test the specificities of anti-ARD1A and anti-ARD1B antibodies on immunoprecipitates pulled down with rabbit anti-HA antibody from transfected cell lysates. **B**) Expression pattern of ARD1A and ARD1B in testes isolated from mice of specified ages. The expression of β-actin was monitored as an internal control. The experiment was repeated, and similar results were obtained.

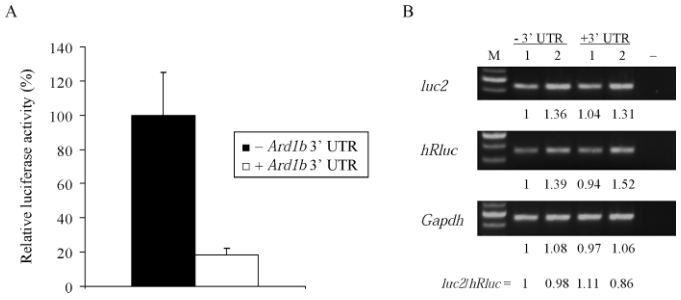

FIG. 5. Repression of luciferase reporter activity in the presence of the *Ard1b* 3′ UTR. **A**) The relative luciferase reporter activity in GC-2spd(ts) cells transfected with reporter constructs in the presence or absence of the *Ard1b* 3′ UTR. Triplicate measurement was performed, and the data shown were the averaged results from three independent experiments. **B**) Determination of transcript levels by RT-PCR of both firefly (*luc2*) and *Renilla* (*hRluc*) luciferase genes in GC-2spd(ts) cells transfected under the same experimental conditions as in **A**. Numerical values represent the relative signal intensities of the PCR products, which were determined using the "Area Density" tool of LabWorks 4.0 (UVP BioImaging Systems). Data presented were obtained from two separate experiments (1 and 2). Amplification of *Gapdh* was performed as an internal control, and its relative signal intensities across all samples are shown. M, DNA ladder; –, no template control. The error bars represent the SDs of the measurement of reporter activity.

for NAT1 used in this study was the same construct as that in the original study [8] and NAT1 alone has been shown not to display NAT activity [8], our results indicate that NAT1-ARD1A or NAT1-ARD1B heterodimer formation is absolutely required for NAT activity and that ARD1B is functionally equivalent to ARD1A in reconstituting an active NAT.

Expression Pattern of ARD1A and ARD1B Proteins During Spermatogenesis

To detect the expression of ARD1B in mouse testes, we generated a rabbit antibody against a unique region close to the C-terminus of the putative protein product. The specificity of the antibody was first tested by Western blotting against an ectopically expressed hemagglutinin (HA)-tagged ARD1B protein in HeLa cells, in which a single immunoreactive band close to the expected size of ARD1B was detected only in cells transiently transfected with ARD1B-HA expression vector (Fig. 4A). Specificity of anti-ARD1A antibody toward only ARD1A-HA protein was similarly observed. Also, both proteins could be detected by anti-HA antibody. In contrast, cells transfected with empty vector or MYC-tagged NAT1 expression vector did not reveal any immunoreactive signal when probed with either anti-ARD1A or anti-ARD1B antibody. We proceeded to perform Western blotting to study the developmental expression patterns of ARD1A and ARD1B during spermatogenesis with whole testicular extracts prepared from 1-day-old, 1-wk-old, 2-wk-old, 3-wk-old, and 2-mo-old mouse testes. ARD1A immunoreactivity was present in all testicular extracts irrespective of the age of animals, presumably owing to the contribution from testicular somatic cells as well (Fig. 4B). In contrast, ARD1B immunoreactivity became detectable only in testicular extract from 3-wk-old mice, and the signal was higher in 2-mo-old mouse testicular extract. The experiment was repeated at a longer exposure time, and the same pattern was obtained (data not shown). During the first wave of spermatogenesis, pachytene spermatocytes and round spermatids first appear in testes of 14-day-old and 21-day-old mice, respectively. Therefore, our results suggest that the transcription and translation processes of *Ard1b* in the mouse testis were uncoupled. Despite the detection of a higher level of *Ard1b* transcripts in pachytene spermatocytes, translation of *Ard1b* would not be initiated until the appearance of round spermatids.

Translational Repression of Ard1b *Is Due to the Presence of the 3′ UTR*

To test if the delayed translation of *Ard1b* in testis would be a result of the presence of the ~2.7-kbp 3′ UTR, we performed a reporter assay by transfecting GC-2spd(ts) cells with reporter constructs with or without the whole 3′ UTR of *Ard1b* immediately downstream of the firefly luciferase gene. For normalization purposes, pGL4.73[*hRluc*/SV40] vector carrying the *Renilla* luciferase gene was cotransfected into these cells. Compared with cells transfected with the parental vector, a significant (~5-fold) reduction of luciferase activity was observed in cells transfected with the *Ard1b* 3′ UTR reporter construct (Fig. 5A), indicating that the presence of the sequence would reduce reporter gene expression. To demonstrate that the reduction in luciferase reporter activity is not a

consequence of lower luciferase transcript expression or a difference in transfection efficiency, a separate experiment was performed to measure the transcript levels of both luciferase genes under the same experimental conditions (Fig. 5B). A similar ratio of the luciferase transcripts was detected in cells transfected with either parental vector or the *Ard1b* 3′ UTR reporter construct. Our data suggest that the reduction of luciferase activity was not due to a decrease in transcript expression or transcript stability; instead, the translation of firefly luciferase was affected.

DISCUSSION

During meiotic sex chromosome inactivation (MSCI), the condensation of X chromosomes leads to cessation of transcription of X-linked genes that often encode housekeeping functions. A continuous presence of the activities of these genes is therefore essential to the completion of spermatogenesis. Retroposition evolved as an important mechanism to generate functional gene duplicates (i.e., retrogenes) in new genomic positions through the RT of expressed progenitor genes [25]. Because autosomes remain transcriptionally active during MSCI, by natural selection X-derived retrogenes would be preserved if they are integrated into autosomes. Many of the X-derived autosomal retrogenes are specifically expressed in the testis [26], with transcription first appearing during or after meiosis [27]. The derivation of retrogenes from their progenitors suggests that the biological activities of their encoded products are similar. Accordingly, the absence of X-derived autosomal retrogene activity has been shown to lead to spermatogenic defects [28–31]. Based on the genomic organization, chromosomal location, tissue and spermatogenic expression pattern, and biochemical function, our results corroborate previous observations [11] that *ARD1B*/*Ard1b* is a bona fide retrogene of *ARD1A*/*Ard1a*. Consistent with the compensation hypothesis [32], the reciprocal expression pattern observed between the two genes during spermatogenesis suggests that *Ard1b* is expressed to compensate for the loss of *Ard1a* starting from meiosis and that NAT activity is crucial to the development of more differentiated male germ cells. However, we do not exclude the possibility that ARD1B may have evolved in parallel a testis-specific role different from that of the ubiquitously expressed ARD1A. Silencing of ARD1A in cell culture by RNAi inhibits cellular proliferation [14, 33] and leads to downregulation of proliferation-promoting genes and upregulation of antiproliferative genes [33]. In another study [8], *Ard1a* was shown to be downregulated upon maturation of mouse neurons; this also occurred when mouse P19 embryonal carcinoma cells were induced to differentiate toward neuronal lineage by retinoic acid. Human ARD1A and NAT1 have been shown to be downregulated upon differentiation in promyelocytic NB4 cells, whereas the level of ARD1B (ARD2) remains constant between undifferentiated and differentiated states [11]. Such evidence suggests a role for ARD1A (presumably with the involvement of NAT1) in cellular proliferation, or their functions are perhaps required only in cells that possess proliferative capacity. Despite that it is functionally homologous to ARD1A, ARD1B is expressed in the mouse at a stage at which male germ cells are not proliferative. Thus, the biological role of ARD1B in testis would be expected to be unrelated to cell growth promotion. Meanwhile, it is also possible that the ARD1A- and ARD1B-associated NAT activities are selective toward different subsets of cellular proteins. Identification of the endogenous substrates of ARD1A and ARD1B would explain if there is a functional difference between the two gene products.

Retrogenes are frequently found to be intronless copies of their progenitors. The extra exon that constitutes the 3′ UTR of *Ard1b* must have been acquired after retroposition [34]. A search of orthologous transcripts from GenBank using the mouse *Ard1b* sequence revealed the same two-exon one-intron genomic structure of the gene in other organisms such as human, chimpanzee, and rat. Conservation of the genomic structure of *Ard1b*/*ARD1B* implies that the 3′ UTR acquisition event should have occurred before the split of primate and rodent lineages. We inspected the retrogenes showing conservation between human and mouse [34] and found that the acquisition process commonly led to the introduction of novel 5′ UTRs. The acquisition of a 3′ exon in *Ard1b*/*ARD1B* is thus an exceptional case. We found that the translation of ARD1B in developing testis was delayed with respect to its transcript expression profile. Our results suggest that ARD1B protein is expressed only after the first appearance of round spermatids in the testis. The uncoupling of gene transcription and translation processes is a strategy commonly used by spermatogenic cell-specific transcripts to ensure their availability for protein translation late in spermiogenesis, when gene transcription is ceased after the compaction of the spermatid genome [35, 36]. It is well known that the 3′ UTR is a harboring site for regulatory elements that affect transcript stability, localization, and translational efficiency [37, 38]. Furthermore, the substantial increase in length of 3′ UTRs in higher eukaryotes appears to correlate with the increase in potential for translational regulation in mammalian cells [39]. These observations led us to hypothesize that the acquired 3′ UTR confers regulatory function on *Ard1b* translation. Accordingly, we observed a significant reduction of luciferase activity when the 2.7-kbp *Ard1b* 3′ UTR was included immediately downstream of the reporter gene in a cell culture model. In fact, regulatory sequence motifs that have been shown to associate with translational repression were identified in the *Ard1b* 3′ UTR, in addition to some uncharacterized regions (Pang et al., unpublished results). The next step would be to study how these elements and the associated factors are involved in suppressing *Ard1b* translation (e.g., by electrophoretic mobility shift assay using testicular extracts from mice of different ages). It would also be helpful to find out if the initiation of ARD1B protein expression is mediated through a switching of distribution of *Ard1b* transcripts from ribonucleoprotein complexes to polysomes in developing male germ cells.

Little is known about the biological significance of N^{α}-terminal acetylation in general or in the context of germ cell development. The expression pattern of ARD1B suggests that its biological action would be exerted late in spermiogenesis. During spermiogenesis, chromatin remodeling occurs in germ cell nuclei to lead to genome compaction before the transformation of spermatids into spermatozoa. Histone (particularly histone H4) hyperacetylation is believed to be an important primer to this remodeling process by facilitating the displacement of histones by protamines [40, 41]. Based on the timing of expression and biochemical properties, the involvement of histone acetyltransferases (HATs) (namely, MYST4 and CDY/CDYL) in testicular histone hyperacetylation is subsequently implicated [42, 43]. HATs are specific to the ε-amino groups of histones. The demonstration of direct acetylation of internal lysine residue(s) of proteins by ARD1A [13, 14] makes it tempting to speculate that ARD1B, which is also shown by confocal microscopy to be localized in the nuclear region (Pang et al., unpublished results), is able to perform similar function on chromatin-associated proteins, including histones. Otherwise, the ARD1B-associated NAT

activity may have a more general biological role in regulating the cascade of biochemical activities in the more differentiated male germ cells. The study of male germ cell development in the absence of ARD1B activity would provide further answers to these biological questions.

ACKNOWLEDGMENT

We would like to thank Roderick A. Corriveau (Department of Cell Biology and Anatomy, Louisiana State University) for the expression constructs CS2+MT-mNAT1, CS2+mARD1/HA, pT7-mNAT1, and pBS-ARD1/HA.

REFERENCES

1. Driessen HP, de Jong WW, Tesser GI, Bloemendal H. The mechanism of N-terminal acetylation of proteins. CRC Crit Rev Biochem 1985; 18:281–325.
2. Polevoda B, Sherman F. N^{α}-terminal acetylation of eukaryotic proteins. J Biol Chem 2000; 275:36479–36482.
3. Polevoda B, Sherman F. Composition and function of the eukaryotic N-terminal acetyltransferase subunits. Biochem Biophys Res Commun 2003; 308:1–11.
4. Gautschi M, Just S, Mun A, Ross S, Rucknagel P, Dubaquie Y, Ehrenhofer-Murray A, Rospert S. The yeast N(alpha)-acetyltransferase NatA is quantitatively anchored to the ribosome and interacts with nascent polypeptides. Mol Cell Biol 2003; 23:7403–7414.
5. Whiteway M, Szostak JW. The ARD1 gene of yeast functions in the switch between the mitotic cell cycle and alternative developmental pathways. Cell 1985; 43:483–492.
6. Mullen JR, Kayne PS, Moerschell RP, Tsunasawa S, Gribskov M, Colavito-Shepanski M, Grunstein M, Sherman F, Sternglanz R. Identification and characterization of genes and mutants for an N-terminal acetyltransferase from yeast. EMBO J 1989; 8:2067–2075.
7. Park EC, Szostak JW. ARD1 and NAT1 proteins form a complex that has N-terminal acetyltransferase activity. EMBO J 1992; 11:2087–2093.
8. Sugiura N, Adams SM, Corriveau RA. An evolutionarily conserved N-terminal acetyltransferase complex associated with neuronal development. J Biol Chem 2003; 278:40113–40120.
9. Arnesen T, Anderson D, Baldersheim C, Lanotte M, Varhaug JE, Lillehaug JR. Identification and characterization of the human ARD1-NATH protein acetyltransferase complex. Biochem J 2005; 386:433–443.
10. Choi SC, Chang JY, Han JK. A novel Xenopus acetyltransferase with a dynamic expression in early development. Biochem Biophys Res Commun 2001; 285:1338–1343.
11. Arnesen T, Betts MJ, Pendino F, Liberles DA, Anderson D, Caro J, Kong X, Varhaug JE, Lillehaug JR. Characterization of hARD2, a processed hARD1 gene duplicate, encoding a human protein N-alpha-acetyltransferase. BMC Biochem 2006; 7:e13.
12. Arnesen T, Gromyko D, Pendino F, Ryningen A, Varhaug JE, Lillehaug JR. Induction of apoptosis in human cells by RNAi-mediated knockdown of hARD1 and NATH, components of the protein N-alpha-acetyltransferase complex. Oncogene 2006; 25:4350–4360.
13. Jeong JW, Bae MK, Ahn MY, Kim SH, Sohn TK, Bae MH, Yoo MA, Song EJ, Lee KJ, Kim KW. Regulation and destabilization of HIF-1alpha by ARD1-mediated acetylation. Cell 2002; 111:709–720.
14. Lim JH, Park JW, Chun YS. Human arrest defective 1 acetylates and activates beta-catenin, promoting lung cancer cell proliferation. Cancer Res 2006; 66:10677–10682.
15. Dym M. Spermatogonial stem cells of the testis. Proc Natl Acad Sci U S A 1994; 91:11287–11289.
16. Schultz N, Hamra FK, Garbers DL. A multitude of genes expressed solely in meiotic or postmeiotic spermatogenic cells offers a myriad of contraceptive targets. Proc Natl Acad Sci U S A 2003; 100:12201–12206.
17. Shima JE, McLean DJ, McCarrey JR, Griswold MD. The murine testicular transcriptome: characterizing gene expression in the testis during the progression of spermatogenesis. Biol Reprod 2004; 71:319–330.
18. Wu SM, Baxendale V, Chen Y, Pang AL, Stitely T, Munson PJ, Leung MY, Ravindranath N, Dym M, Rennert OM, Chan WY. Analysis of mouse germ-cell transcriptome at different stages of spermatogenesis by SAGE: biological significance. Genomics 2004; 84:971–981.
19. Chan WY, Lee TL, Wu SM, Ruszczyk L, Alba D, Baxendale V, Rennert OM. Transcriptome analyses of male germ cells with serial analysis of gene expression (SAGE). Mol Cell Endocrinol 2006; 250:8–19.
20. Pang ALY, Johnson W, Ravindranath N, Dym M, Rennert OM, Chan WY. Expression profiling of purified male germ cells: stage-specific expression patterns related to meiosis and postmeiotic development. Physiol Genomics 2006; 24:75–85.
21. Kozak M. An analysis of 5′-noncoding sequences from 699 vertebrate messenger RNAs. Nucleic Acids Res 1987; 15:8125–8148.
22. Burset M, Seledtsov IA, Solovyev VV. Analysis of canonical and non-canonical splice sites in mammalian genomes. Nucleic Acids Res 2000; 28:4364–4375.
23. Chun KH, Cho SJ, Choi JS, Kim SH, Kim KW, Lee SK. Differential regulation of splicing, localization and stability of mammalian $ARD1^{235}$ and $ARD1^{225}$ isoforms. Biochem Biophys Res Commun 2007; 353:18–25.
24. Eddy EM. Male germ cell gene expression. Recent Prog Horm Res 2002; 57:103–128.
25. Long M, Betrán E, Thornton K, Wang W. The origin of new genes: glimpses from the young and old. Nat Rev Genet 2003; 4:865–875.
26. Emerson JJ, Kaessmann H, Betran E, Long M. Extensive gene traffic on the mammalian X chromosome. Science 2004; 303:537–540.
27. Wang PJ. X chromosomes, retrogenes and their role in male reproduction. Trends Endocrinol Metab 2004; 15:79–83.
28. Miki K, Qu W, Goulding EH, Willis WD, Bunch DO, Strader LF, Perreault SD, Eddy EM, O'Brien DA. Glyceraldehyde 3-phosphate dehydrogenase-S, a sperm-specific glycolytic enzyme, is required for sperm motility and male fertility. Proc Natl Acad Sci U S A 2004; 101: 16501–16506.
29. Bradley J, Baltus A, Skaletsky H, Royce-Tolland M, Dewar K, Page DC. An X-to-autosome retrogene is required for spermatogenesis in mice. Nat Genet 2004; 36:872–876.
30. Rohozinski J, Bishop CE. The mouse juvenile spermatogonial depletion (jsd) phenotype is due to a mutation in the X-derived retrogene, mUtp14b. Proc Natl Acad Sci U S A 2004; 101:11695–11700.
31. Rohozinski J, Lamb DJ, Bishop CE. UTP14c is a recently acquired retrogene associated with spermatogenesis and fertility in man. Biol Reprod 2006; 74:644–651.
32. McCarrey JR, Thomas K. Human testis-specific PGK gene lacks introns and possesses characteristics of a processed gene. Nature 1987; 326:501–505.
33. Fisher TS, Etages SD, Hayes L, Crimin K, Li B. Analysis of ARD1 function in hypoxia response using retroviral RNA interference. J Biol Chem 2005; 280:17749–17757.
34. Vinckenbosch N, Dupanloup I, Kaessmann H. Evolutionary fate of retroposed gene copies in the human genome. Proc Natl Acad Sci U S A 2006; 103:3220–3225.
35. Braun RE. Post-transcriptional control of gene expression during spermatogenesis. Semin Cell Dev Biol 1998; 9:483–489.
36. Hecht NB. Molecular mechanisms of male germ cell differentiation. Bioessays 1998; 20:555–561.
37. de Moor CH, Meijer H, Lissenden S. Mechanisms of translational control by the 3′ UTR in development and differentiation. Semin Cell Dev Biol 2005; 16:49–58.
38. Hughes TA. Regulation of gene expression by alternative untranslated regions. Trends Genet 2006; 22:119–122.
39. Mazumder B, Seshadri V, Fox PL. Translational control by the 3′-UTR: the ends specify the means. Trends Biochem Sci 2003; 28:91–98.
40. Grimes SR Jr, Henderson N. Hyperacetylation of histone H4 in rat testis spermatids. Exp Cell Res 1984; 152:91–97.
41. Meistrich ML, Trostle-Weige PK, Lin R, Bhatnagar YM, Allis CD. Highly acetylated H4 is associated with histone displacement in rat spermatids. Mol Reprod Dev 1992; 31:170–181.
42. Lahn BT, Tang ZL, Zhou J, Barndt RJ, Parvinen M, Allis CD, Page DC. Previously uncharacterized histone acetyltransferases implicated in mammalian spermatogenesis. Proc Natl Acad Sci U S A 2002; 99: 8707–8712.
43. McGraw S, Morin G, Vigneault C, Leclerc P, Sirard MA. Investigation of MYST4 histone acetyltransferase and its involvement in mammalian gametogenesis. BMC Dev Biol 2007; 7:e123.